LAND DEGRADATION & DEVELOPMENT
Land Degrad. Develop. **28**: 1386–1397 (2017)
Published online 23 November 2016 in Wiley Online Library (wileyonlinelibrary.com) **DOI**: 10.1002/ldr.2608

SUITABILITY OF WATERSHED MODELS TO PREDICT DISTRIBUTED HYDROLOGIC RESPONSE IN THE AWRAMBA WATERSHED IN LAKE TANA BASIN

Mamaru A. Moges[1,2], Petra Schmitter[3], Seifu A. Tilahun[1], Simon Langan[3], Dessalegn C. Dagnew[2], Adugnaw T. Akale[2], Tammo S. Steenhuis[1,4]*

[1]*Faculty of Civil and Water Resources Engineering, Bahir Dar Institute of Technology, Bahir Dar University, Bahir Dar, Ethiopia*
[2]*PhD Program in Integrated Water Management, Bahir Dar Institute of Technology, Bahir Dar University, Bahir Dar, Ethiopia*
[3]*International Water Management Institute (IWMI), East Africa and Nile Basin Office, Addis Ababa, Ethiopia*
[4]*Departments of Biological and Environmental Engineering, Cornell University, Ithaca, NY 14853, USA*

Received 13 February 2016; Revised 26 August 2016; Accepted 26 August 2016

ABSTRACT

Planning effective landscape interventions is an important tool to fight against land degradation and requires knowledge on spatial distribution of runoff. The objective of this paper was to test models that predict temporal and spatial distribution of runoff. The selected models were parameter-efficient semi-distributed watershed model (PED-WM), Hydrologiska Byrans Vattenbalansavdelning integrated hydrological modeling system (HBV-IHMS), and Soil and Water Assessment Tool (SWAT). We choose 7-km^2 Awramba watershed in the Lake Tana basin with detailed hydrological information for testing these models. Discharge at the outlet, rainfall, and distributed information on infiltration rates, water table, and extent of the saturated area were collected from 2013 to 2015. The maximum saturated area was 6·5% of the watershed. Infiltration rates exceeded rainfall intensities 91% of the time. Hence, saturation excess runoff was the main runoff mechanism. Models were calibrated for the rainy seasons in 2013 and 2014 and validated for 2015. For daily flow validation, the PED-WM model (Nash–Sutcliff efficiency, NSE = 0·61) outperformed HBV-IHMS (NSE = 0·51) and SWAT (NSE = 0·48). Performance on monthly time step was similar. Difference in model behavior depended on runoff mechanism. In PED-WM, saturation excess is the main direct runoff process and could predict the maximum extent of the saturated area closely at 6·9%. HBV-IHMS model runoff simulation depended on soil moisture status and evapotranspiration, and hence was able to simulate saturation excess flow but not the extent of the saturated area. SWAT, where infiltration excess is the main runoff mechanism, could only predict the monthly discharges well. This study shows that prevailing runoff mechanisms and distribution of runoff source areas should be used for proper model selection. Copyright © 2016 John Wiley & Sons, Ltd.

KEY WORDS: catchment hydrology; distributed hydrology modeling; land degradation; saturation excess; Lake Tana basin

INTRODUCTION

Land degradation is a worldwide concern (Bridges & Oldeman, 1999; Meadows & Hoffman, 2002; Wessels *et al*., 2004) that requires new approaches to counteract its effects. It is becoming a threat for developing countries like Ethiopia, where it decreases agricultural productivity (Taddese, 2001; Zeleke & Hurni, 2001; Nyssen *et al*., 2004; Bishaw, 2005; Assefa & Hans, 2015). However, finding innovative solutions is hampered by data scarcity and watershed models that have not been tested for monsoon and mountainous climates. The availability of suitable and climate specific watershed models can aid in accurately predicting runoff and sediment loads from watersheds and hence provide support in planning of sustainable natural resource management interventions without further degrading the land (Bisantino *et al*., 2015; Borrelli *et al*., 2015; Gessesse *et al*., 2015).

Suitable watershed model development, for better understanding the change in rainfall–runoff relationships due to anthropogenic influences at watershed scale, has been of interest over the past decades (Duan *et al*., 1992; Jakeman & Hornberger, 1993; Johnson *et al*., 2003). A wealth of watershed models conceptualizing different rainfall–runoff process has been developed and tested in different parts of the world (Knebl *et al*., 2005; Keesstra *et al*., 2009). These models represent a wide variety of spatio-temporal resolution, complexity, data, and computational requirement aside from their individual limitations (Johnson *et al*., 2003; Sorooshian *et al*., 2008).

One of the major tasks in developing watershed models is the simulation of rainfall partitioning into infiltration and runoff. This depends on a unique set of watershed features (e.g., topography, geomorphology, soil type, and land use) (Hernandez *et al*., 2000; Brooks *et al*., 2012) and the spatio-temporal variation of precipitation determined by the regional climate (Hewlett & Hibbert, 1967; Fohrer *et al*., 2001; VanShaar *et al*., 2002; Legesse *et al*., 2003; Sikka *et al*., 2003; Merritt *et al*., 2006; Schaefli *et al*., 2010; Chung *et al*., 2011). As such, hydrological and sedimentation processes are not uniform within the landscape, and models able to represent the physical linkage between the different components and their connectivity at the watershed scale are preferred (Masselink *et al*., 2016).

*Correspondence to: T. S. Steenhuis, Departments of Biological and Environmental Engineering, Cornell University, Ithaca, NY 14853, USA.
E-mail: tss1@cornell.edu

Watershed hydrological models can be categorized in several groups, depending on its model structure, conceptualization, and spatio-temporal resolution: (i) empirical models (e.g., artificial neural network (ANN); Kisi, 2004: Antar *et al*., 2006), genetic programming (Meshgi *et al*., 2015) and unit hydrograph (Nash, 1957); (ii) conceptual models [e.g., Hydrologiska Byrans Vattenbalansavdelning integrated hydrological modeling system (HBV-IHMS); Bergström & Singh, 1995], TOPModel (Beven *et al*., 1984), Stanford Watershed Model (SWM) (Crawford & Linsley, 1966), and ARNO (Todini, 1996); (iii) physically based [e.g., Soil and Water Assessment Tool (SWAT); Arnold *et al*., 1998], MIKE -Système Hydrologique Européen (MIKE-SHE) (DHI, 1998), AGricultural Non-Point Source pollution model (AGNPS) (Young *et al*., 1996), Chemicals, Runoff, and Erosion from Agricultural Management Systems (CREAMS) (Knisel, 1980), and parameter-efficient semi-distributed watershed model (PED-WM; Steenhuis *et al*., 2009); and (iv) a hybrid combining two or more types i to iii (Wheater *et al*., 1986; Devia *et al*., 2015). Additionally, models can be categorized as lumped (e.g., artificial neural network; Kisi, 2004; Antar *et al*., 2006), SACramento (Burnash, 1995), or distributed (e.g., SWAT, MIKE-SHE, PED-WM, and HBV-IHMS). When evaluating their rainfall–runoff process conceptualization, a distinction between (i) saturation excess (e.g., PED-WM) and (ii) infiltration excess or Hortonian overland flow (e.g., SWAT) can be made for physically distributed models, whereas for non-physically based models, it depends on how the hybrid, empirical, or conceptual functions were obtained (Johnson *et al*., 2003).

The suitability and accuracy of these models partially depend on how well model input parameters describe the relevant watershed characteristics (FitzHugh & Mackay, 2000) and connectivity of processes within the watershed (Masselink *et al*., 2016). As such, the dominating runoff generation mechanism can be evaluated for a particular watershed based on model performance, as this is strongly related to the models' rainfall–runoff concept in combination with overall watershed observations (Sivapalan, 2003).

In the Blue Nile basin, several conceptual and physical watershed models were used: MIKE Basin (Mulat & Moges, 2014), PED-WM (Collick *et al*., 2009; Steenhuis *et al*., 2009; Tilahun *et al*., 2012, 2013a; Guzman *et al*., 2013), HBV-IHMS (Wale *et al*., 2009; Rientjes *et al*., 2011), and SWAT (Mekonnen *et al*., 2009; Setegn *et al*., 2009a, 2010; Bitew & Gebremicheal, 2011; Kaleab & Manoj, 2013). Each of the models has been applied separately based on data availability, computational capacity, license, and expertise and subsequently calibrated and validated by using standard statistical model performance indicators.

However, watershed models' comparison and suitability based on distributed watershed observations and rainfall–runoff mechanisms have not been studied so far in the Ethiopian Highlands. Comparing predicted and observed runoff source areas yields insight in the type of runoff processes and the strength of models in simulating watersheds in the highlands. Particularly, this study is aimed at comparing the suitability of the various models in Lake Tana basin in order to realistically simulate the runoff processes to implement management practices such as soil conservation practices in agricultural watersheds within the basin. Particularly, this study is aimed at comparing the suitability of the various models to realistically simulate runoff both at the outlet and spatially. Unlike discharge predictions where a drop of water at the outlet from anywhere in the watershed is the same, the location of surface runoff generation is important for properly modeling of non-point source pollution and optimum placement of soil and water conservation practices. For example, in the New York water supply source watershed, where saturation excess runoff (similar to the Ethiopian Highlands) dominates, water quality was greatly improved by management practices that reduced the nutrient input in the periodically saturated areas (Rao *et al*., 2009). Similarly, targeting soil and water conservation that are directed to infiltrate runoff to the areas that do not become saturated and check dams to those that become saturated will significantly increase the effectiveness of soil and water conservation practices (Tebebu *et al*., 2015), improve farm income (Erkossa *et al*., 2015), aid toward restoring natural vegetation and carbon cycle management (Batjes, 2014), and safeguard the multi-purpose Lake Tana from being degraded by non-point source pollution. The objective of this study was twofold: (i) understand the main drivers behind runoff generation from field observations and (ii) evaluate those findings through comparison of overall model performance and runoff source area comparison for three differently defined rainfall–runoff models. The study was conducted in the Awramba watershed (7 km^2), one of the representative watersheds draining to Lake Tana. The evaluation of model-based predictions on the spatial distribution of the hydrological sensitive areas (i.e., runoff-generating areas) yields important information for best management practices. This can be used in the region to optimize gully rehabilitation, as gully formation is most severe in the periodically saturated bottom lands.

MATERIALS AND METHODS

Description of Study Area

The study was conducted in Awramba watershed (11° 55·765′–11°55·765′N and 37°47·539′–37°47·539′E, 1887–2291 m asl), a 7-km^2 micro-watershed (Figure 1). It is located in the south east of Lake Tana, 75 km to the northwest of Bahir Dar town. The river from the Awramba watershed drains into the Ribb River (main tributary to Lake Tana). The monitored watershed is ideal, as its topography represents the complexity of the Ethiopian Highlands with their undulated, depression, and flat surfaces. The climate in the watershed can be characterized as sub-humid monsoonal. The average temperature is around 22 °C in January and 19 °C in July. The annual average rainfall during the main rainy season (June to September) is 1,098 mm. The soils are from volcanic origin and mainly clayey throughout the

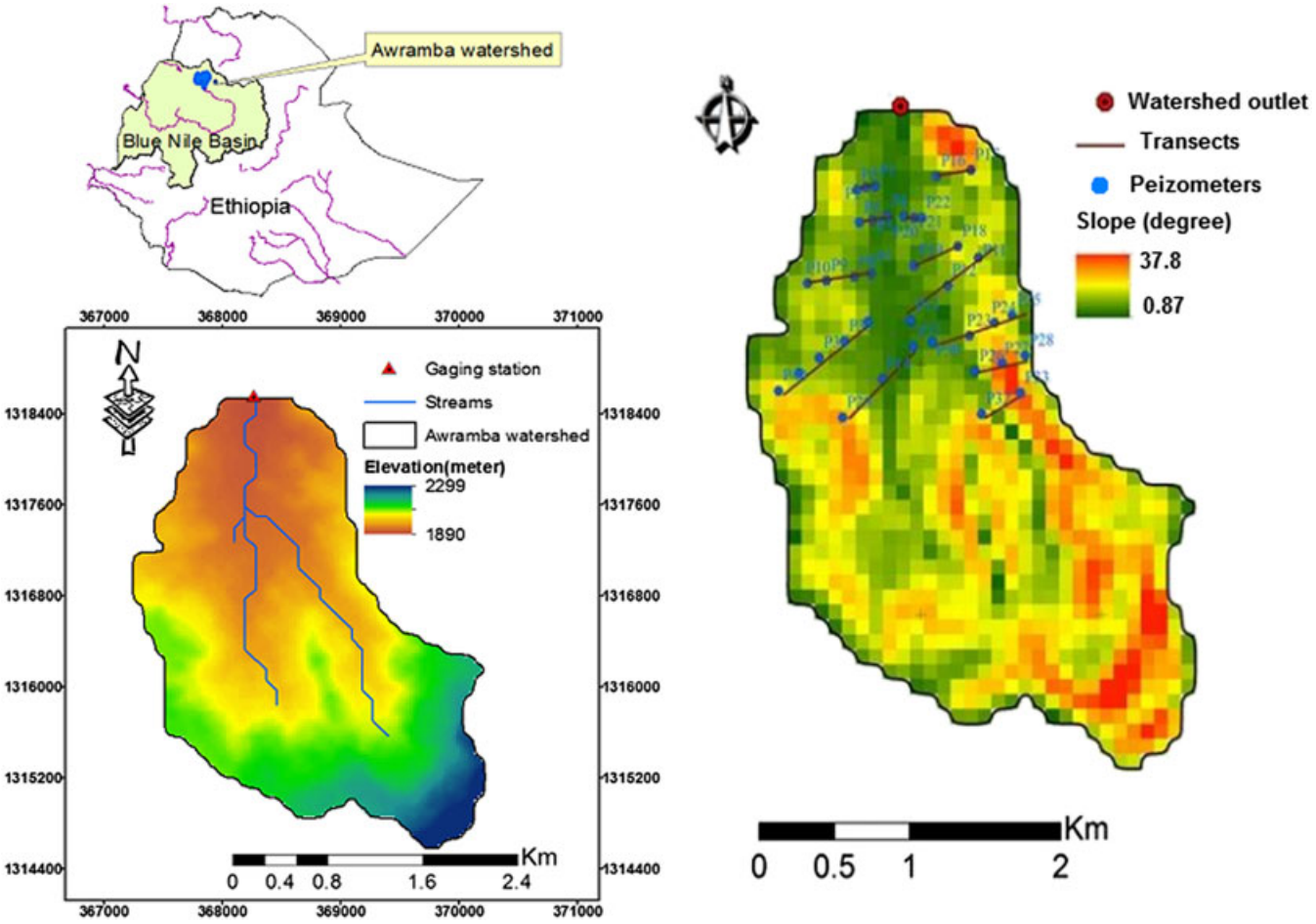

Figure 1. Location and geographical positions of the Awramba watershed (left) with the spatial distribution of the piezometers in the watershed (right). [Colour figure can be viewed at wileyonlinelibrary.com]

mid and downslope positions and clay to sandy clay on the top slopes. The downslope part of the watershed is mainly covered by grassland, with few agricultural patches and evergreen trees on the river banks. The mid slope/hillside part of the watershed is mainly used for cultivation of teff and maize. As part of a country wide campaign on soil and water conservation, the communities in the watershed have implemented stone bunds and terraces at the mid slope part of the watershed since 2010.

Hydro-Meteorological Data Collection in the Watershed

Rainfall data were collected automatically in the rainy seasons of 2013, 2014, and 2015 by using the automatic tipping bucket rain gauge (*e+rain WatchDog*).The rainfall was recorded with an accuracy of 0·1 mm and a temporal resolution of 5 min. Groundwater tables in the watershed were measured through the installation of 39 piezometers (PVC pipes, with a diameter of 50 mm) perpendicular to the stream. The length of the installed piezometers varied from 1·1 m (rocky degraded areas of the watershed) up to 3·1 m in shallow soils. From a total of 39 piezometers, 10 were installed at the top slope, 12 mid slope, and 17 downslope positions in the watershed. Water levels were recorded manually each morning in the rainy seasons of 2013, 2014, and 2015.

Infiltration rates, using a 25 cm diameter single ring infiltrometer, were measured at different locations representing various topographic positions and land use types within the watershed. The measurements were distributed equally among the three distinct landscapes of the watershed and repeated thrice. A total of 21 measurements were carried out at the bottom slope, hillside, and top slope part of the watershed. Steady state infiltration rate at the end of the measurement similar with Wang *et al*. (2015) and Cerdá (1999) was taken as the infiltration capacity of the respective topographic position.

The gauging station for flowing water level measurements was located at the outlet of the watershed (11°55·765′N, 37° 47·539′E; Figure 1a). A broad-crested weir was constructed, and flow depth was manually measured twice a day by using the staff gauge. Velocity was measured thrice at low, medium, and peak flows by using a current meter. Discharge was computed by using the velocity–area method in order to establish a stage discharge rating curve as power function with an $R^2 = 0{\cdot}97$ (Figure S1).

Watershed Models

Three watershed models – namely PED-WM, HBV-IHMS, and SWAT – were used to simulate runoff process in the Awramba watershed. Each of the models uses a different

rainfall–runoff generation concept and thus requires distinct spatio-temporal and hydro-meteorological data sets (Table S1) for calibration and validation (Table I).

PED-WM

In the PED-WM, a daily time step semi-distributed watershed model, saturation excess runoff principles were taken into account (Steenhuis *et al*., 2009; Tessema *et al*., 2010). Within the model, the watershed is divided into three zones: two zones producing surface runoff and one zone contributing to the interflow and baseflow of the watershed. The defined surface runoff areas are the valley bottoms, where saturation occurs during the main rainy season, and degraded hillsides having a slowly permeable sub-horizon at a shallow soil depth. The hillsides, where the rainwater infiltrates and either contributes to interflow (zero-order reservoirs) or baseflow (first-order reservoir), are grouped together in the third zone. The model computes for each zone a water balance where the rest term is excess water, Q_{sr} (Equation 1a–b). The excess, when greater than zero, is designated surface runoff for the saturated and the degraded zones and percolation (eventually becoming interflow and baseflow) for the third zone.

$$Q_{sr} = 0 \ \text{When} \ S_t \leq S_{max} \tag{1a}$$

Otherwise,

$$Q_{sr} = P_t + \frac{S_{t-\Delta t} - S_{max}}{\Delta t} - ET_t \tag{1b}$$

Where: Q_{sr} = runoff, P = precipitation (mm/day), and ET_t = actual evapotranspiration (mm/day) and is calculated by using the Thornthwaite–Mather (Steenhuis & van der Molen, 1986): Δt is the time step (day), S_t is the storage at time t, and S_{max} (mm) is the maximum amount of water that can be held in the root zone = change in moisture storage (mm), with the temporal scale of daily monthly and annual resolution.

The model has nine main parameters: the area fraction (A) and the maximum storage capacity (S_{max}) for the three zones. Additionally, to compute the quick subsurface interflow and baseflow, three subsurface parameters are used: the drainage time of the zero-order (interflow) reservoir (τ^*) and the half-life ($t_{1/2}$) of the first-order (baseflow) reservoir with a maximum storage capacity (B_{Smax}). Detailed description about the model can be found from Tesemma *et al*. (2010) and Tilahun *et al*. (2013a, 2013b).

HBV-IHMS

The HBV-IHMS, a daily time step watershed model (Bergström & Singh, 1995; Lindström *et al*., 1997), is a semi-distributed conceptual rainfall runoff model (Equation 2). The model allows dividing the catchment into sub-basins and further into elevation and vegetation zones. The model consists of subroutines for snow accumulation and melt, soil moisture accounting procedure, routines for runoff generation, and a simple routing procedure. The soil moisture routine is controlled by precipitation, actual evapotranspiration, and field capacity. Groundwater recharge starts when the soil moisture exceeds field capacity, whereas runoff is computed when excess soil moisture is generated. The model computes the runoff and water balance

Table I. Calibrated parameters for three watershed models in the Awramba watershed

Model	PSR	Parameter	Description of the parameter	Parameter range		Optimum fitted parameter
				Max	Min	
	1	A_h	Portion of hillside area (%)			72
	2	$S_{max,s}$	Maximum soil water storage(mm) in A_s			150
	3	*	Interflow(days)			20
	4	Bs_{max}	Maximum storage for baseflow(mm) linear reservoir			100
PED-W	5	A_d	Portion of degraded area (%)			12·0
	6	A_s	Portion of saturated area (%)			6·94
	7	$t_{1/2}$	Baseflow half life time(days)			8
	8	$S_{max,d}$	Maximum soil water storage in A_d			230
	9	$S_{max,h}$	Maximum soil water storage(mm) in A_h			35
	1	F_c	Field capacity(mm)	100	500	120
	2	Beta	Exponent in formula for drainage from soil	0	1	0·4
	3	Alpha*	Discharge calculating exponent in the upper zone	0·5	1·1	0·74
HBV-IHMS	4	lp	Limit for potential evapotranspiration	0	1	0·7
	5	hq*	Calculated parameter from catchment	—	—	1·2
	6	K4	Recession coefficient of lower response box	0	0·1	0·0637
	7	Perc	Percolation from the upper response box (mm day^{-1})	0·01	6	0·3
	1	Cn2	Initial SCS-CN II value	−0·2	0·2	−0·134
	2	Ch_K2	Effective hydraulic conductivity	5	130	111·625
	3	Alpha_Bnk	Baseflow alpha factor for bank storage	0	1	0·139
	4	Ch_n2	Manning roughness for main channel	0	0·2	0·0705
SWAT	5	Gwqmn	Threshold depth of water in shallow aquifer required for return flow	0	2	1·502
	6	Sol_Bd	Moist soil bulk density	−0·5	0·5	−0·0039
	7	Gw_Delay	Groundwater delay time	30	450	369·78
	8	Sol_k	Soil hydraulic conductivity	−0·8	0·8	0·1808

components at sub-basin level which is subsequently routed through the watershed providing the outlet discharge. Sub-basin classification in HBV-IHMS model was based on the intersection of mean elevation and vegetation cover in the watershed. After classifying the elevation into four mean elevation zones and vegetation (as forest and field), the two reclassified maps were overlaid and six sub-basins were identified for HBV-IHMS modeling. The water balance equation used at sub-basin level for the Awramba watershed was:

$$Q_{sr} = P_{\Delta t} - ET_{\Delta t} + \frac{\Delta SM + \Delta UZ + \Delta LZ}{\Delta t} \quad (2)$$

Where: all quantities are taken over a time period of Δt, Q_{sr} is discharge at the outlet, $P_{\Delta t}$ is precipitation, ΔSM is change in soil moisture, ΔUZ is change in upper groundwater zone, ΔLZ is change in lower groundwater zone, and $ET_{\Delta t}$ is actual evapotranspiration. Detailed description of the model can be found from HBV-IHMS manual version 5·1 (SMHI, 2005).

SWAT

The SWAT, developed by Arnold *et al*. (1998), is a semi-distributed physically based watershed model where the watershed is subdivided into sub-basins containing a variety of homogenous hydrologic response units (HRUs). The subdivision of HRU is based on elevation, soil type, management, and land use/cover types. The model simulation starts at HRU level. Surface runoff is computed by using the Soil Conservation Services Curve Number method and occurs whenever the effective rainfall exceeds the rate of infiltration. For each HRU, runoff is calculated and routed to obtain the total runoff for the watershed outlet. The watershed was divided into 3 sub-basins and 14 HRUs by SWAT. The soil and land use maps had a scale of 1:20000. The water balance component of the model is described by using the following mathematical description:

$$Q_{sr} = \sum_{i=1}^{n} \left(\frac{\left(P - ET - DP - Q_{gw} + \frac{\Delta S}{\Delta t}\right) A_i}{\sum_{i=1}^{n} A_i} \right) \quad (3)$$

Where: Q_{sr} is the discharge at the outlet, ΔS is the change in moisture content in the ith HRU, Δt is 1 day, P is daily precipitation, ET is daily evaporation, DP is the amount of deep percolation, and Q_{gw} is the groundwater flow from the ith HRU. All units are in mm or mm day^{-1}. A detailed description of the model can be found from SWAT model documentation (Neitsch *et al*., 2011).

Sensitivity and Calibration of Rainfall Runoff Models

The hydro-meteorological data collected in the rainy season of 2013 and 2014 were used as calibration, whereas 2015 was used for validation. For each model, sensitivity analysis was carried out to obtain the most sensitive parameters controlling the rainfall–runoff process. The one-factor-at-a-time principle (Morris, 1991; Van *et al*., 2006) was used for both manual (i.e., PED-WM and HBV-IHMS) and automatic sensitivity procedures (SWAT). For PED-WM and HBV-IHMS, sensitive parameters were identified by increasing or decreasing each parameter manually by 10% while others were kept constant, whereas for SWAT, the one-factor-at-a-time (LATIN-hypercube one-factor-at-a-time (LH-OAT)) module in the SWAT-CUP-2 version 5·1 was used. The Sequential Uncertainty Fitting version 2 algorithm was used for sensitivity analysis and to identify parameters for further optimization. The watershed model performances were evaluated by using common model efficiency measuring criteria, that is, the Nash–Sutcliff efficiency (NSE; Nash and Sutcliff, 1970).

Runoff Areas at Watershed Scale

Monitored groundwater levels and community discussion were used to map runoff sources in the watershed. Delineation of these areas was compared against the "activated" runoff areas from the respective models. In the PED-WM model, the total area was obtained by calibrating the discharge at the outlet and the location was found by using the topographic wetness index (TWI; Ambroise *et al*., 1996; Sivapalan *et al*., 1987; Lyon *et al*., 2005; Agnew *et al*., 2006; Bayabil *et al*., 2010). For HBV-IHMS and SWAT, the runoff source areas were based on the watershed discretization, evaluating the runoff from sub-basins in HBV-IHMS and HRUs for SWAT.

Identification of Runoff Areas Using Mapping Tools

Identification of runoff areas at watershed scale was performed by using two methods. The first method – applicable for small watersheds – combined community-based mapping with field observations, whereas the second method made use of the TWI, a method easily applicable for larger watersheds.

Community-based saturation area mapping took place at the onset of the rainy season and was complemented by using the daily water level measurements from the piezometers. Areas where water level rose quickly following precipitation and maintained high for a significant period of time after the event were mapped by using a Global Positioning System (GPS). The groundwater level data obtained from the piezometer readings were combined with the community mapping to draw the delineation of the hydrological sensitive or high runoff source areas.The TWI method made use of a digital elevation model of 30 m resolution (http://earthexplorer.usgs.gov/) according to:

$$\lambda = \ln\left(\frac{aR}{\tan(\beta) K_S D}\right) \quad (4)$$

Where: λ is the topographic index [units of ln(d/m)], a is upslope contributing area per unit contour length (m), tan (β) is the local surface topographic slope, K_S is the mean saturated hydraulic conductivity of the soil (m/day), D is the soil depth (m), and R is the average recharge rate. Because of limited information, K_S, D, and R were kept constant throughout the watershed.

Model Identified Runoff Source Areas

The identification of the runoff generating areas in the PED-WM models can be derived from model calibrated parameter (fraction of saturated area). However, the PED-WM model is not fully distributed. The location of the runoff areas was therefore derived by using the TWI, as the PED-WM model is based on topographic zonation. In order to validate the runoff source area from the model output, mapping of periodically saturated areas in the rainy season was tracked by using Global Positioning System and the area was mapped and analyzed in ARCGIS 10·1 software.

The delineation of the runoff generating areas from the HBV-IHMS was carried out at sub-basin level, as these are the smallest units (Table S2). Firstly, runoff was separated from the simulated stream flow by using the baseflow-to-stream flow ratio. Subsequently, the most sensitive land use and topographic areas contributing to runoff were ranked (i.e., higher rank was given to the lowest mean elevation and agricultural land use, and the lowest was given to higher mean elevation and forest land use. Finally, the runoff index was mapped by multiplying the rank with the ratio of runoff volume from each sub-basin with the total runoff volume from the watershed.

The runoff source area in SWAT was obtained by evaluating the amount of runoff generated from each HRU (Table S3) by using ARCGIS 10·1. The runoff obtained from each HRU in each sub-basin was weighted through division by the total watershed runoff volume. The total runoff obtained from each sub-basin was multiplied by the area of each HRU and divided by the total area of the watershed. The runoff source index raster map was developed by converting the runoff volume from HRUs with the total runoff volume from the watershed area.

RESULTS AND DISCUSSION

First, the physical attributes of the watershed are examined in order to define whether saturation excess or infiltration excess runoff is more likely to occur. This was carried out by plotting rainfall intensities versus median infiltration rates and examining the depth of water tables throughout the watershed. Subsequently, model suitability for the Awramba watershed in the Lake Tana basin was assessed by first comparing the predicted and observed discharge at the outlet and subsequently matching the observed versus predicted runoff source areas.

Runoff Mechanism Based on Field Observations

Rainfall intensity and infiltration rate

The rainfall intensities in the 2013, 2014, and 2015 rain phase in the watershed varied between 2·4 and 116 mm h^{-1} with an average of 7·5 mm h^{-1}. Maximum infiltration rates of 90 mm h^{-1} were found at the mid slope position of the watershed. In the valley bottoms where the soils are saturated, lowest infiltration rates of 7·5 mm h^{-1} were observed. This was consistent with similar studies conducted in the Ethiopian Highlands where infiltration rates are limited in saturated soils (Bayabil *et al*., 2010; Tilahun *et al*., 2014). The majority of low infiltration rates were found downslope, while some were measured on the severely degraded soils mid slope. The median infiltration was 30 mm h^{-1} (Bayabil *et al*., 2010; Engda *et al*., 2011; Tilahun *et al*., 2014). From the total 668 recorded precipitation events, rainfall intensity exceeded the median infiltration rate of 30 mm h^{-1} only 9% of the time (Figure 2), which was similar to the results obtained for Maybar watershed (1·13 km^2) by Bayabil *et al*. (2010).

Groundwater table

The water table in the downslope piezometers (10) rose nearly to the surface in early August and remained at the surface (i.e., 250 cm below the soil surface) till the end of September after which levels declined slowly for both 2013 and 2014 (Figure 3a and b). Groundwater levels measured at the mid slope piezometers (P8, P9, P11, P19, and P20; Figure 1) remained below the surface and declined earlier and faster than those measured in the saturated area (groundwater level data not shown). This clearly indicates that the majority of rainfall drained via interflow from up- to downslope resulting in saturation of the foot slopes given its relatively smaller slope.

Model Performance Based on Runoff Mechanism

The three watershed models were evaluated on predicting temporal distribution of discharge at the outlet and the spatial distribution of runoff generating areas with the watershed. The year 2013 and 2014 were used for calibration and 2015 for validation (Table II) for both daily and monthly time steps. Inferences are made on the most suitable runoff mechanisms for this watershed.

Difference in Model Sensitivity to Rainfall–Runoff Generation at the Watershed Outlet

In PED-WM, manual sensitivity analysis for discharge at the outlet resulted in the identification of four most sensitive

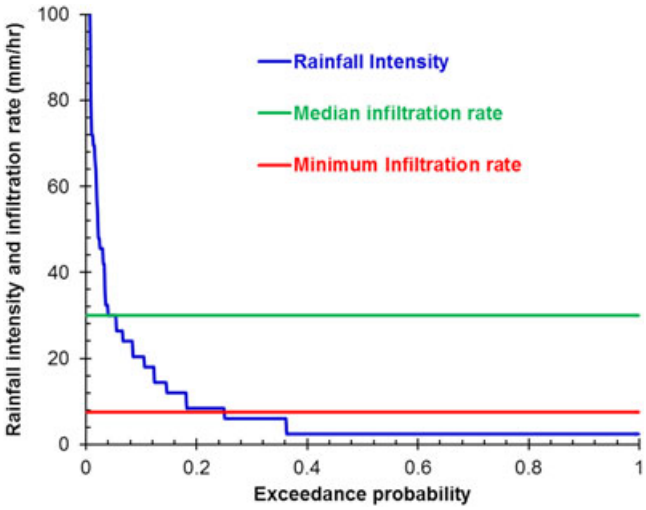

Figure 2. Exceedance probabilities of rainfall intensity with medium and minimum infiltration rates for the Awramba watershed. [Colour figure can be viewed at wileyonlinelibrary.com]

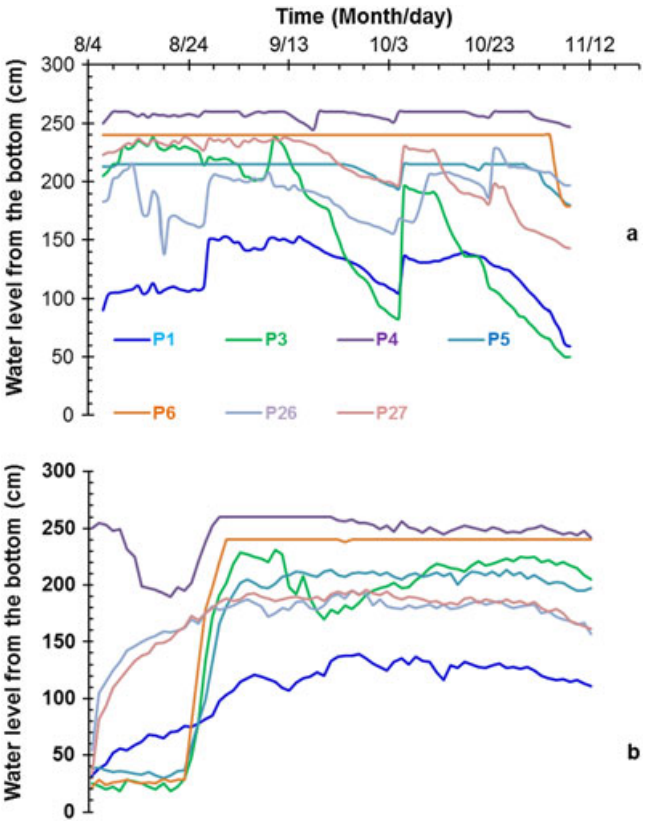

Figure 3. Groundwater level readings in the lower part of the Awramba watershed for (a) 2013 and (b) 2014. [Colour figure can be viewed at wileyonlinelibrary.com]

parameters: the areal hillside coverage (A_h), the saturated area (A_S), maximum soil storage in the saturated area (S_{max}), and the recession coefficient (k; Figure 4a).

Hydrologiska Byrans Vattenbalansavdelning integrated hydrological modeling system originally had more than 30 parameters of which only seven model parameters control the total volume and shape of the hydrograph (Wale *et al*., 2009). Out of those seven parameters, four were found to be most sensitive: field capacity (f_c), parameter for soil drainage (β), discharge parameter (α), and the limit for evapotranspiration (lp; Figure 4b).

From the 13 SWAT parameters identified by Setegn *et al*. (2010) for Lake Tana basin, eight parameters were found most sensitive in the runoff generation for Awramba watershed (Table I). From these eight

Table II. Model performance during calibration (2013–2014) and validation (2015) at the outlet of Awramba watershed

Calibration/ validation	Model	Performance value (NSE)	
		Daily	Monthly
Calibration	PED-W	0·64	0·91
	HBV-IHMS	0·54	0·91
	SWAT	0·5	0·91
Validation	PED-W	0·61	0·92
	HBV-IHMS	0·5	0·88
	SWAT	0·48	0·92

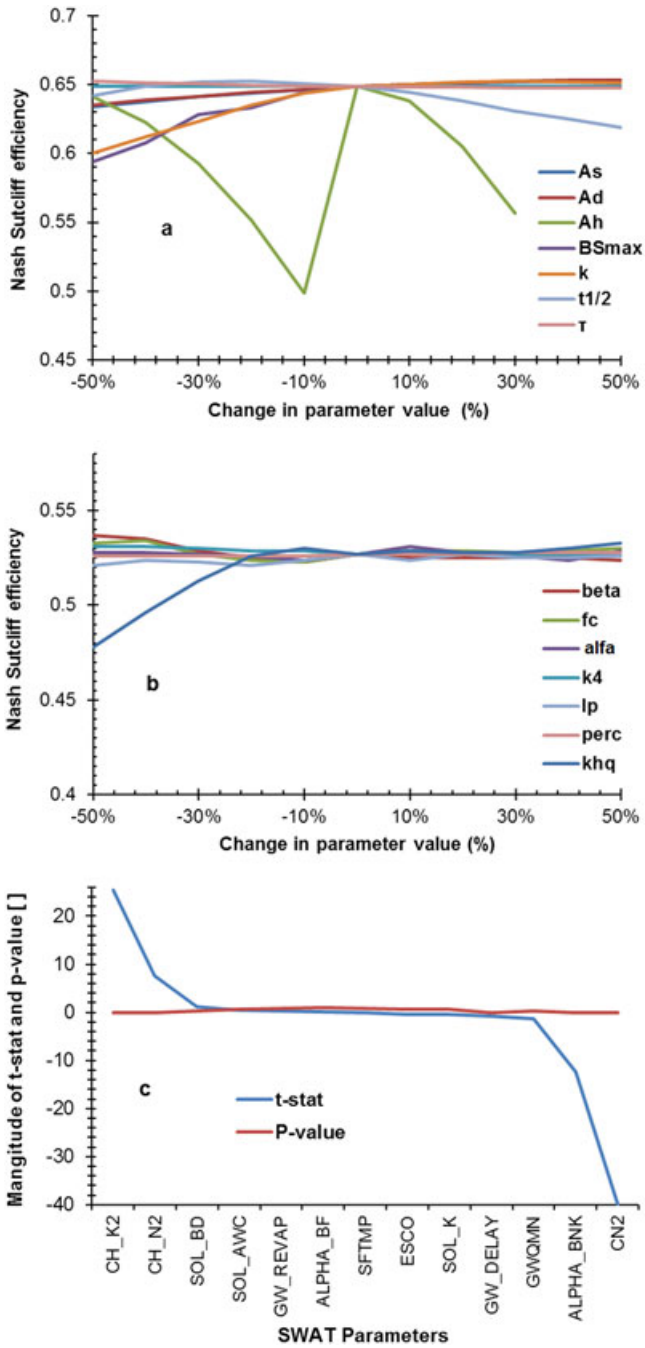

Figure 4. Model sensitivity results for (a) parameter-efficient semi-distributed watershed model (PED-WM), (b) Hydrologiska Byrans Vattenbalansavdelning integrated hydrological modeling system (HBV-IHMS), and (c) Soil and Water Assessment Tool (SWAT). [Colour figure can be viewed at wileyonlinelibrary.com]

parameters, the following four were identified as most sensitive: initial curve number (Soil Conservation Services Curve Number II, CN2), effective hydraulic conductivity (CH_K2), baseflow alpha factor for bank storage (ALPHA_BNK), and channel manning roughness (CH_N2) (Figure 4c). The sensitivity of the curve number parameter was consistent with other studies in Upper Blue Nile basin (Mekonnen *et al*., 2009; Setegn *et al*., 2009a, 2010; Bitew & Gebremicheal, 2011; Kaleab & Manoj, 2013; Ali *et al*., 2014).

From the model sensitivity, it seems that the most sensitive parameters in PED-WM and HBV were related to either fast or slow release of soil moisture from storage, whereas for SWAT, it was mainly the curve number of the principal parameter in Hortonian overland flow runoff and a set of parameters to slow down the Hortonian flow so it would last over several days.

Model Rainfall–Runoff Generation Performance at the Outlet

At a daily time step, the observed discharge was simulated by using PED-WM with NSEs of 0·64 and 0·61 whereas for HBV-IHMS NSE was 0·54 and 0·5 and for SWAT 0·5 and 0·48 during calibration and validation periods, respectively (Figures 5a–c and 6, Table II). Model performance at a monthly time step showed similar results for the three models in the calibration period (NSE = 0·91), and the NSE ranged from 0·88 to 0·92 in the validation period (Table II). The results are within the range of similar studies: PED-WM

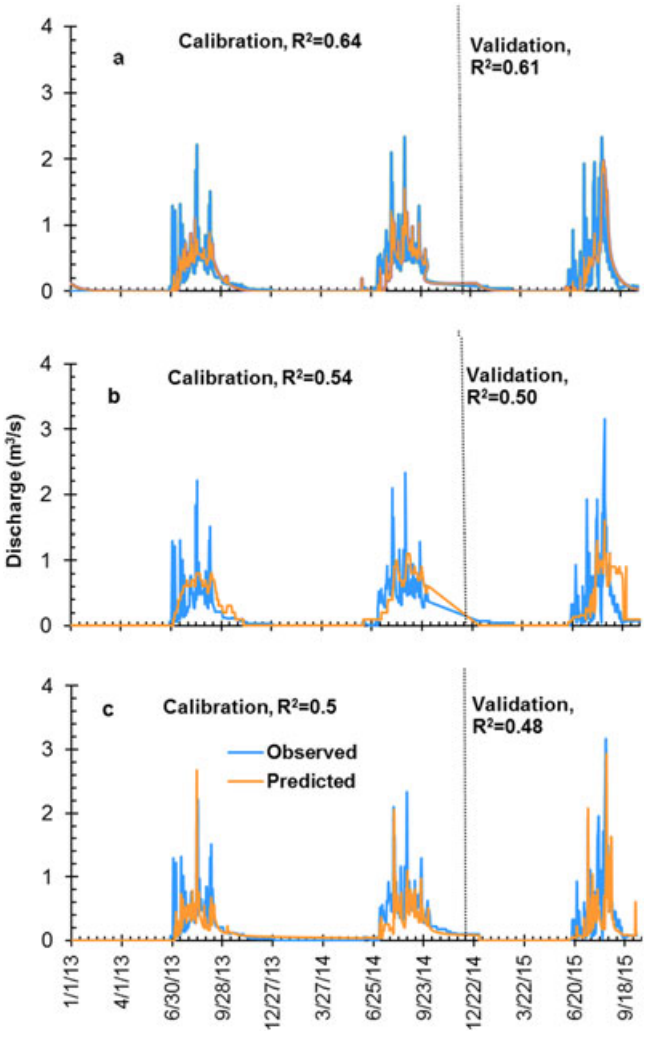

Figure 5. Daily predicted and observed discharge for the Awramba watershed during calibration (2013–2014) and validation (2015) for (a) PED-WM, (b) HBV-IHMS, and (c) SWAT. [Colour figure can be viewed at wileyonlinelibrary.com]

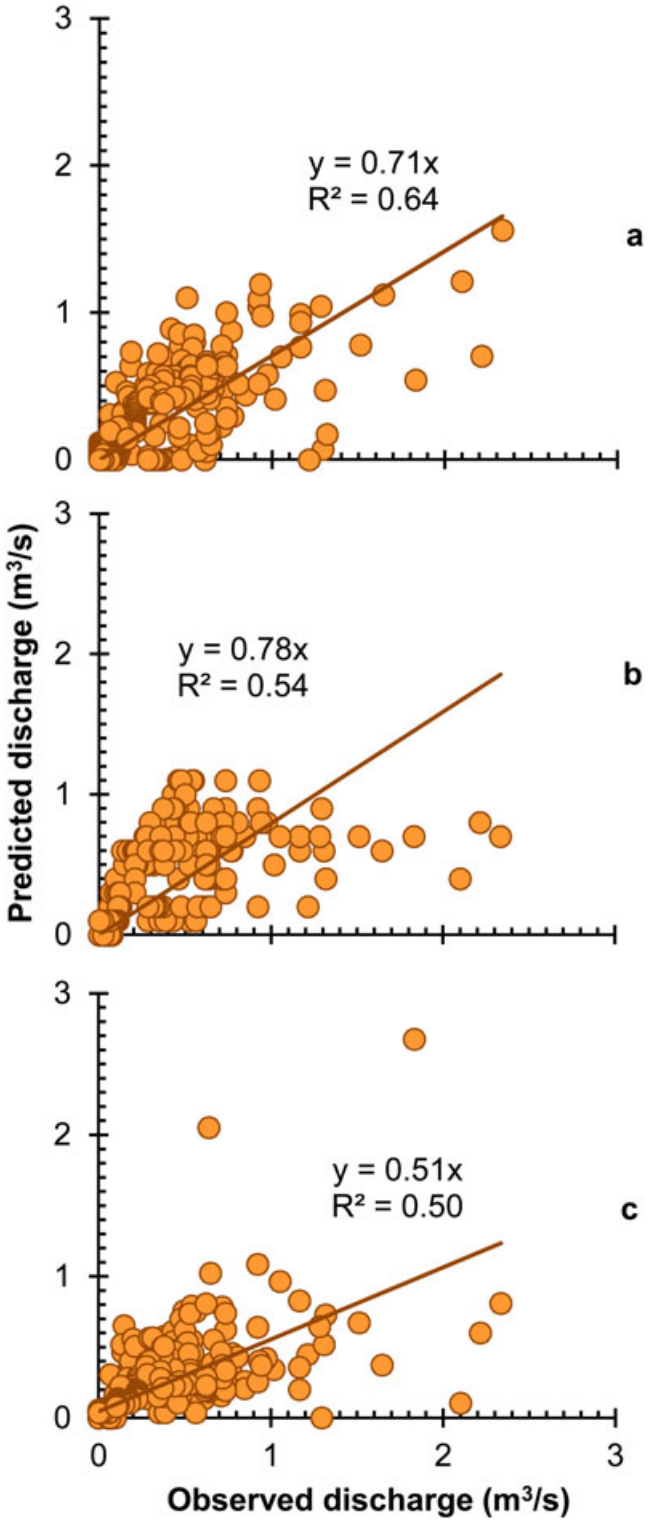

Figure 6. Daily predicted and observed discharge for the Awramba watershed during calibration (2013–2014) for (a) PED-WM, (b) HBV-IHMS, and (c) SWAT. [Colour figure can be viewed at wileyonlinelibrary.com]

(Collick *et al*., 2009; Steenhuis *et al*., 2009; Tesamma *et al*., 2010; Tilahun *et al*., 2013a, 2013b, 2015), HBV-IHMS (Wale *et al*., 2009; Rientjes *et al*., 2011), and SWAT by Setegn *et al*. (2009a) for Gumara (1274 km^2) and Ribb (1288 km^2) watersheds (in which the Awramba watershed

is located) and Easton *et al.* (2010) for the upper Blue Nile basin at Kessi (165,000 km^2).

The calibrated parameters in the PED-WM model showed that direct runoff at the outlet originated from saturated area (constituting 6·9% of the watershed) and degraded slopes (12%; Table I). In the remaining part of the watershed, the rain infiltrated contributing to inter- and baseflow (Table I). This was in accordance with field observations of interflow draining most of the watershed with limited overland flow on the hill slopes. The HBV model overestimated the baseflow and underestimated peak discharge. Unlike the PED-WM, where overland flow is simulated as a delta function, HBV uses continuous functions. This makes it difficult for HBV to simulate sharp peak discharges at the outlet, especially in micro watersheds. Hence, HBV might be slightly less suitable for daily discharge predictions in the Awramba watershed (Figure 5b).

The SWAT model underpredicted the runoff for a vast majority of rainfall events. This is directly related to the curve number method in SWAT which assumes a relationship between rainfall and discharge, independent of the stage of the rain phase (Betrie *et al.*, 2011). It could, therefore, not simulate the increasing runoff ratio from almost zero in the beginning of the rainfall season to over 50% later in the rainy phase (Tilahun *et al.*, 2016).

In all cases, monthly discharge values were predicted well by all three models (Table II, Figures 7a–c). Because timing of the surface runoff becomes insignificant at a larger time scale, all three models essentially perform as a water balance model that assigns a certain portion to baseflow. Because model calibration included baseflow parameters, models should perform similarly.

Runoff Source Areas

Through the integration of community discussions with groundwater table readings, saturated areas were mapped. The saturation areas were found near the outlet of the watershed (delineated with a black line in Figure 8a). The saturated area had its largest extent in August and accounted for 6·5% of the total watershed area, which is equivalent to a land area of 44 ha. TWI map was prepared by ranking the calculated indices from high (wet) to low (dry; Figure 8a). The blue-colored area has the greatest TWI and coincided well with saturated areas (delineated black line, in Figure 8a). The PED-WM model predicted closely the areal coverage of the runoff source area (value of A_s, Table I). By using the TWI values to map the saturated areas as proposed by Lyon *et al.* (2004) and Schneiderman *et al.* (2007), runoff areas coincided with the observed saturated areas (Figure 8a).

Runoff source areas predicted by HBV-IHM were based on the amount of simulated overland flow. The greater the runoff, the more likely the area was saturated. The HBV-IHMS model predicted correctly that most runoffs were generated in the valley bottom (Figure 8b) but could not pinpoint exactly the observed saturated area (Figure 8a).

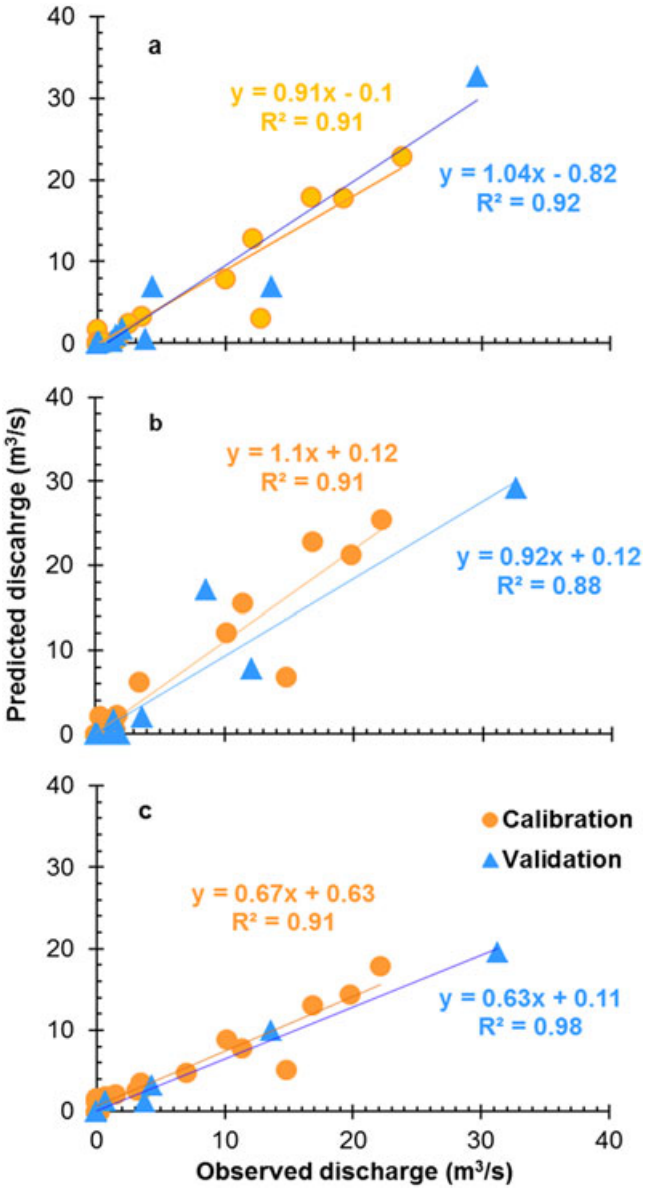

Figure 7. Monthly predicted and observed discharge for the Awramba watershed during calibration (2013–2014) and validation (2015) for (a) PED-WM, (b) HBV-IHMS, and (c) SWAT. [Colour figure can be viewed at wileyonlinelibrary.com]

Soil and Water Assessment Tool, as expected, simulates more runoff from the hillsides with the greatest curve number values followed by the mid slope (Figure 8c). Unlike the other models, SWAT simulates the least amount of runoff in the bottom part of watershed area.

Generally, the basic assumption for runoff generation in PED-WM was in line with groundwater observations, infiltration measurements, and rainfall intensities observed in the watershed during 2013 to 2015. Similarly, the HBV-IHMS watershed model indicated that in the valley bottoms the highest runoff was generated. SWAT, in which the runoff is generated by a combination of soil and plant conditions independent of the landscape position, could not simulate the saturation excess runoff in the valley bottom of the watershed.

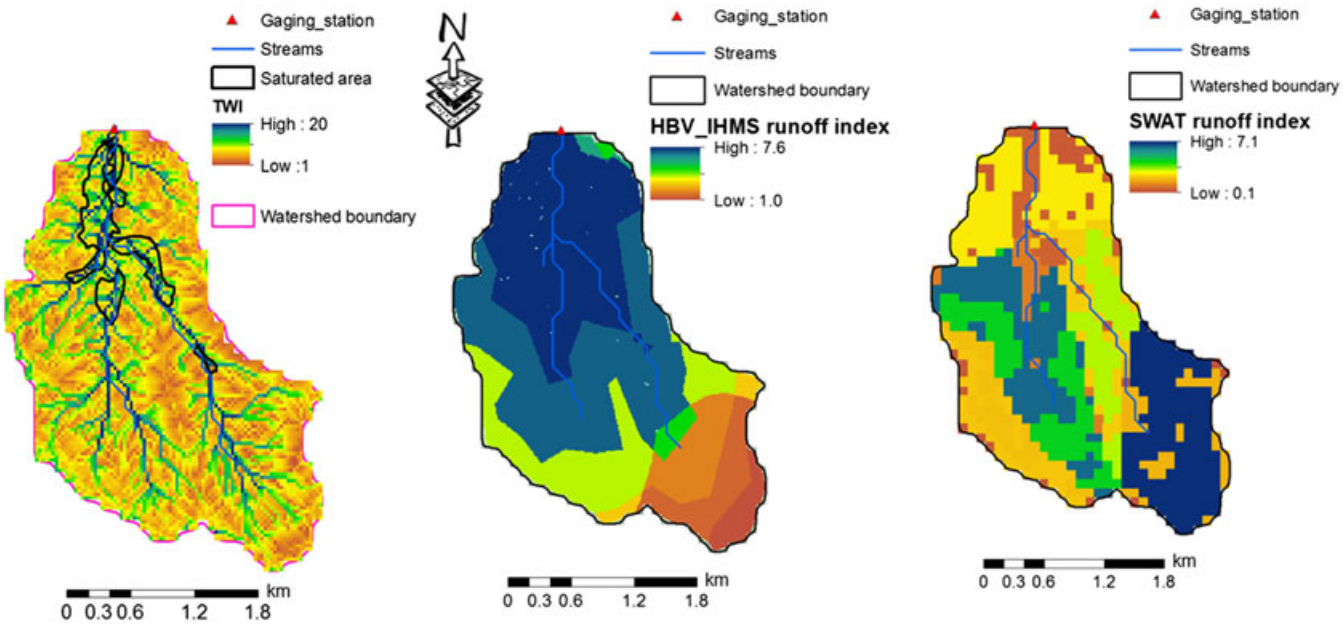

Figure 8. Runoff source areas identified by the various hydrological semi-distributed watershed models: (a) the black polygons referring to PED-WM source areas overlaid with topographic wetness index map, (b) HBV-IHMS, and (c) SWAT. [Colour figure can be viewed at wileyonlinelibrary.com]

CONCLUSION

Three watershed models were tested in the Awramba watershed in the Lake Tana basin where direct runoff was generated mainly by saturation excess. Both the predicted temporal discharge at the outlet and spatial locations of the runoff source areas were compared with observed measurement. The PED-WM (a semi-distributed saturation excess runoff model) was relatively accurate in predicting the discharge at the outlet and the location of the runoff source areas. HBV-IHM was next best, while SWAT, based on infiltration excess, could only simulate discharges at a monthly time step and was not capable of locating the runoff source areas in the valley bottom. For non-point source watershed models where the location of runoff source areas is important for identifying the optimum location of natural resource management practices, identifying the type of runoff beforehand is of paramount importance. We found that the Lake Tana basin, saturation excess models such as the PED-WM, will perform best for this purpose.

ACKNOWLEDGEMENTS

This research was sponsored in part by the USAID through the research project “Participatory Enhanced Engagement in Research” or PEER Science project (grant no. AID-OAA-A-11-00012). Additional funding was also obtained from Higher Education for Development (HED), United States Department of Agriculture (USDA), Innovation Laboratory for Small Scale Irrigation project (no. AID-OAA-A-13-000SS) funded by Feed the Future through the US Agency for International Development, International Science Foundation (IFS) in Sweden, and funds provided by Cornell University partly through the highly appreciated gift of an anonymous donor.

REFERENCES

Agnew LJ, Lyon S, Gérard MP, Collins VB, Lembo AJ, Steenhuis TS, Walter MT. 2006. Identifying hydrologically sensitive areas: bridging the gap between science and application. *Journal of Environmental Management* **78**(1): 63–76. DOI:10.1016/j.jenvman.2005.04.021.

Ali YS, Crosato A, Mohamed YA, Abdalla SH, Wright NG. 2014. Sediment balances in the Blue Nile river basin. *International Journal of Sediment Research* **29**(13): 316–328. DOI:10.1016/S1001-6279(14)60047-0.

Ambroise B, Beven K, Freer J. 1996. Toward a generalization of the TOPMODEL concepts: topographic indices of hydrological similarity. *Journal of Water Resource Research* **32**(7): 2135–2145. DOI:10.1029/95WR03715.

Antar MA, Elassiouti I, Mohammed NA. 2006. Rainfall–runoff modeling using artificial neural networks technique: a Blue Nile catchment case. *Hydrological Processes* **20**(5): 1201–1216. DOI:10.1002/hyp.5932.

Arnold JG, Srinivasan R, Muttiah RS, Williams JR. 1998. Large area hydrologic modeling and assessment part I: model development1, Wiley Online Library. *Journal of the American Water Resources Association* **34**(1): 73–89. DOI:10.1111/j.1752-1688.1998.tb05961.x.

Assefa E, Hans RB. 2015. Farmers' perception of land degradation and traditional knowledge in Southern Ethiopia—resilience and stability. *Land Degradation & Development* . DOI:10.1002/ldr.2364.

Batjes NH. 2014. Projected changes in soil organic carbon stocks upon adoption of recommended soil and water conservation practices in the Upper Tana river catchment, Kenya. *Land Degradation and Development* **25**(3): 278–287. DOI:10.1002/ldr.2141.

Bayabil HK, Tilahun SA, Collick AS, Yitaferu B, Steenhuis TS. 2010. Are runoff processes ecologically or topographically driven in the (sub) humid Ethiopian Highlands? The case of the Maybar watershed. *Ecohydrology* **3**(4): 457–466. DOI:10.1002/eco.170.

Bergström S, Singh V. 1995. The HBV model. *Computer Models of Watershed Hydrology* : 443–476 ISBN 0-918334-91-8.

Betrie G, Mohamed Y, Griensven AV, Srinivasan R. 2011. Sediment management modeling in the Blue Nile basin using SWAT model. *Hydrology and Earth System Sciences* **15**: 807–818. DOI:10.5194/hess-15-807-2011.

Beven KJ, Kirkby MJ, Schofield S, Tagg AF. 1984. Testing a physically-based flood forecasting model (TOPMODEL) for three U.K. catchments.

Journal of Hydrology **69**(1-4): 119–143. DOI:10.1016/0022-1694(84)90159-8.

Bishaw B. 2005. Deforestation and land degradation in the Ethiopian Highlands: a strategy for physical recovery. *Northeast African Studies* **8**(1): 7–25. DOI:10.1353/nas.2005.0014.

Bitew MM, Gebremichael M. 2011. Evaluation of satellite rainfall products through hydrologic simulation in a fully distributed hydrologic model. *Water Resources Research* **47**(6): 1–11. DOI:10.1029/2010WR009917.

Bisantino T, Bingner R, Chouaib W, Gentile F, Trisorio LG. 2015. Estimation of runoff, peak discharge and sediment load at the event scale in a medium-size Mediterranean watershed using the AnnAGNPS model. *Land Degradation and Development* **26**(4): 340–355. DOI:10.1002/ldr.2213.

Borrelli P, Märker M, Schütt B. 2015. Modeling post-tree-harvesting soil erosion and sediment deposition potential in the Turano river basin (Italian Central Apennine). *Land Degradation and Development* **26**(4): 356–366. DOI:10.1002/ldr.2214.

Bridges EM, Oldeman LR. 1999. Global assessment of human-induced soil degradation. *Arid Soil Research and Rehabilitation* **13**(4): 319–325.

Brooks KN, Folliott PF, Magner JA. 2012. *Hydrology and the management of watersheds*. John Wiley and Sons: Ames, Iowa, USA.

Burnash RJC. 1995. The NWS River Forecast System—catchment modeling. In *Computer models of watershed hydrology*, Singh VP (ed). Water Resources Publications: Highlands ranch, Colorado, U.S.A; 311–366. ISBN:0-918334-91-8.

Cerdà A. 1999. Seasonal and spatial variations in infiltration rates in badland surfaces under Mediterranean climatic conditions. *Water Resources Research* **35**(1): 319–328. DOI:10.1029/98WR01659.

Chung ES, Park K, Lee KS. 2011. The relative impacts of climate change and urbanization on the hydrological response of a Korean urban watershed. *Hydrological Processes* **25**(4): 544–560. DOI:10.1002/hyp.7781.

Collick AS, Easton ZM, Ashagrie T, Biruk B, Tilahun SA, Adgo E, Awulachew SB, Zeleke G, Steenhuis TS. 2009. A simple semi-distributed water balance model for the Ethiopian Highlands. *Hydrological Processes* **23**: 3718–3727. DOI:10.1002/hyp.7517.

Crawford NH, Linsley RK. 1966. Digital simulation in hydrology Stanford Watershed Model 4IV (SWM) Stanford University.

Devia GK, Ganasri BP, Dwarakish GS. 2015. A review on hydrological models. *Aquatic Procedia* **4**: 1001–1007. DOI:10.1016/j.aqpro.2015.02.126.

Danish Hydraulic Institute. 1998. MIKE-SHE version 5·3 user guide and technical reference manual, Danish Hydraulic Institute, Denmark.

Duan Q, Sorooshian S, Gupta V. 1992. Effective and efficient global optimization for conceptual rainfall–runoff models. *Water Resources Research* **28**(4): 1015–1031. DOI:10.1029/91WR02985.

Easton ZM, Fuka DR, White ED, Collick AS, Biruk AB, McCartney M, Awulachew SB, Ahmed AA, Steenhuis TS. 2010. A multi basin SWAT model analysis of runoff and sedimentation in the Blue Nile, Ethiopia. *Hydrological and Earth System Science* **14**: 1827–1841. DOI:10.5194/hess-14-1827-2010.

Engda TA, Bayabil HK, Legesse ES, Ayana EK, Tilahun SA, Collik AS, Easton ZM, Rimmer A, Awulachew SB, Steenhuis TS. 2011. Watershed hydrology of the (semi) humid Ethiopian Highlands. In *Nile river basin hydrology*. Springer: New York.

Erkossa T, Wudneh A, Desalegn B, Taye G. 2015. Linking soil erosion to on-site financial cost: lessons from watersheds in the Blue Nile basin. *Solid Earth* **6**(2): 765–774. DOI:10.5194/se-6-765-2015.

FitzHugh TW, Mackay D. 2000. Impacts of input parameter spatial aggregation on an agricultural nonpoint source pollution model. *Journal of Hydrology* **236**(1–2): 5–53. DOI:10.1016/S0022-1694(00)00276-6.

Fohrer N, Haverkamp S, Eckhardt K, Frede HG. 2001. Hydrologic response to land use changes on the catchment scale. *Physics and Chemistry of the Earth, Part B: Hydrology, Oceans and Atmosphere* **26**(7): 577–582. DOI:10.1016/S1464-1909(01)00052-1.

Gessesse B, Bewket W, Bräuning A. 2015. Model-based characterization and monitoring of runoff and soil erosion in response to land use/land cover changes in the Modjo Watershed, Ethiopia. *Land Degradation and Development* **26**(7): 711–724. DOI:10.1002/ldr.2276.

Guzman CD, Tilahun SA, Zegeye AD, Steenhuis TS. 2013. Suspended sediment concentration–discharge relationships in the (sub-) humid Ethiopian Highlands. *Hydrology and Earth System Sciences* **17**(3): 1067–1077. DOI:10.5194/hess-17-1051-2013.

Hernandez M, Miller SN, Goodrich DC, Goff BF, Kepner GM, Edmonds CK, Bruce JB. 2000. Modeling runoff response to land cover and rainfall spatial variability in semi-arid watersheds. In *Monitoring ecological condition in the western United States*, Springer: Netherlands; 285–298. DOI:10.1007/978-94-011-4343-1_23.

Hewlett JD, Hibbert AR. 1967. Factors affecting the response of small watersheds to precipitation in humid areas. *Forest Hydrology* **1**: 275–290.

Jakeman AJ, Hornberger GM. 1993. How much complexity is warranted in a rainfall-runoff model? *Water Resource Research* **29**: 2637–2649. DOI:10.1029/93WR00877.

Johnson MS, Coon WF, Mehta VK, Steenhuis TS, Brooks ES, Boll J. 2003. Application of two hydrologic models with different runoff mechanisms to a hill slope dominated watershed in the northeastern US: a comparison of HSPF and SMR. *Journal of Hydrology* **284**: 57–76. DOI:10.1016/j.jhydrol.2003.07.005.

Kaleab MM, Manoj KJ. 2013. Runoff and sediment modeling using SWAT in Gumera catchment, Ethiopia. *Open Journal of Modern Hydrology* **3**: 196–206. DOI:10.4236/ojmh.2013.34024.

Keesstra SD, Bruijnzeel LA, van Huissteden J. 2009. Meso-scale catchment sediment budgets: combining field surveys and modeling in the Dragonja catchment. *Southwest Slovenia Earth Surface Processes and Landforms* **34**: 1547–1561. DOI:10.1002/esp.1846.

Kisi Ö. 2004. River flow modeling using artificial neural networks. *Journal of Hydrologic Engineering* **9**(1): 60–63. DOI:10.1061/(ASCE)1084-0699(2004)9:1(60).

Knebl MR, Yang ZL, Hutchison K, Maidment DR. 2005. Regional scale flood modeling using NEXRAD rainfall, GIS, and HEC-HMS/RAS: a case study for the San Antonio river basin summer 2002 storm event. *Journal of Environmental Management* **75**(4): 325–336. DOI:10.1016/j.jenvman.2004.11.024.

Knisel WG. 1980. CREAMS: a field-scale model for chemicals, runoff and erosion from agricultural management systems. USDA Conservation Research Report 26.

Legesse D, Vallet CC, Gasse F. 2003. Hydrological response of a catchment to climate and land use changes in Tropical Africa: case study South Central Ethiopia. *Journal of Hydrology* **275**(1): 67–85. DOI:10.1016/S0022-1694(03)00019-2.

Lindström G, Johansson B, Persson M, Gardelin M, Bergström S. 1997. Development and test of the distributed HBV-96 hydrological model. *Journal of Hydrology* **201**: 272–288. DOI:10.1016/S0022-1694(97)00041-3.

Lyon SW, Seibert J, Lembo AJ, Walter MT, Steenhuis TS. 2005. Geostatistical investigation into the temporal evolution of spatial structure in a shallow water table. *Hydrology and Earth System Sciences Discussions* **2**(4): 1683–1716 Hal-00298696.

Lyon SW, Walter MT, Gérard MP, Steenhuis TS. 2004. Using a topographic index to distribute variable source area runoff predicted with the SCS curve-number equation. *Hydrological Processes* **18**(15): 2757–2771. DOI:10.1002/hyp.1494.

Masselink RJH, Keesstra SD, Temme AJAM, Seeger M, Giménez R, Casalí J. 2016. Modeling discharge and sediment yield at catchment scale using connectivity components. *Land Degradation and Development* **27**(4): 933–945. DOI:10.1002/ldr.2512.

Meadows ME, Hoffman MT. 2002. The nature, extent and causes of land degradation in South Africa: legacy of the past, lessons for the future? *Area* **34**(4): 428–437. DOI:10.1111/1475-4762.00100.

Mekonnen MA, Worman A, Dargahi B, Gebeyehu A. 2009. Hydrological modeling of Ethiopian catchments using limited data. *Hydrological Processes* **23**: 3401. DOI:10.1002/hyp.7470.

Merritt WS, Alila Y, Barton M, Taylor B, Cohen S, Neilsen D. 2006. Hydrologic response to scenarios of climate change in sub watersheds of the Okanagan basin, British Columbia. *Journal of Hydrology* **326**(1): 79–108. DOI:10.1016/j.jhydrol.2005.10.025.

Meshgi A, Schmitter P, Chui TFM, Babovic V. 2015. Development of a modular streamflow model to quantify runoff contributions from different land uses in tropical urban environments using genetic programming. *Journal of Hydrology* **525**: 711–723. DOI:10.1016/j.jhydrol.2015.04.032.

Morris MD. 1991. Factorial sampling plans for preliminary computational experiments. *Technimetrics* **33**(2): 161–174. DOI:10.2307/1269043.

Mulat AG, Moges SA. 2014. Assessment of the impact of the Grand Ethiopian Renaissance Dam on the performance of the High Aswan Dam. *Journal of Water Resource and Protection* **6**(6). DOI:10.4236/jwarp.2014.66057.

Nash J, Sutcliffe J. 1970. River flow forecasting through conceptual models part IA discussion of principles. *Journal of Hydrology* **10**: 282–290. DOI:10.1016/00221694(70)90255-6.

Nash J. 1957. The form of the instantaneous unit hydrograph. *International Association of Scientific Hydrology* **3**: 114–121.

Neitsch SL, Arnold JG, Kinir JR, William JR. 2011. Soil and Water Assessment Tool theoretical documentation version 2009. Grassland, Soil and

Water Research Laboratory, Agricultural Research Service, Backland Research Center, Texas AgriLife Research.
Nyssen J, Poesen J, Moeyersons J, Deckers J, Mitiku H, Lang A. 2004. Human impact on the environment in the Ethiopian and Eritrean Highlands state of the art. *Earth Science Reviews* **64**(3): 273–320. DOI:10.1016/S0012-8252(03)00078-3.
Rao NS, Easton ZM, Schneiderman EM, Zion MS, Lee DR, Steenhuis TS. 2009. Modeling watershed-scale effectiveness of agricultural best management practices to reduce phosphorus loading. *Journal of Environmental Management* **90**: 1385–1395. DOI:10.1016/j.jenvman.2008.08.011.
Rientjes T, Perera B, Haile A, Reggiani PP, Muthuwatta L. 2011. Regionalization for lake level simulation—the case of Lake Tana in the upper Blue Nile, Ethiopia. *Hydrology and Earth System Sciences* **15**: 1167–1183. DOI:10.5194/hess-15-1167-2011.
Schaefli B, Harman CJ, Sivapalan M, Schymanski SJ. 2010. Hydrologic predictions in a changing environment: behavioral modeling. *Hydrology and Earth System Sciences Discussions* **7**(5): 7779–7808. DOI:10.5194/hessd-7-7779-2010.
Schneiderman EM, Steenhuis TS, Thongs DJ, Easton ZM, Zion MS, Neal AL, Todd WM. 2007. Incorporating variable source area hydrology into a curve-number-based watershed model. *Hydrological Processes* **21**(25): 3420–3430. DOI:10.1002/hyp.6556.
Setegn SG, Srinivasan R, Dargahi B. 2009a. Hydrological modeling in the Lake Tana Basin, Ethiopia using SWAT model. *Open Hydrology Journal* **2**: 49–62. DOI:10.2174/1874378100802010049.
Setegn SG, Srinivasan R, Melesse AM, Dargahi B. 2010. Swat model application and prediction uncertainty analysis in the Lake Tana basin, Ethiopia. *Hydrological Processes* **24**: 357–367. DOI:10.1002/hyp.7457.
Sikka AK, Samra JS, Sharda VN, Samraj PP, Lakshmanan V. 2003. Low flow and high flow responses to converting natural grassland into bluegum (*Eucalyptus globulus*) in Nilgiris watersheds of South India. *Journal of Hydrology* **270**(1): 12–26. DOI:10.1016/S0022-1694(02)00172-5.
Sivapalan M. 2003. Process complexity at hill slope scale, process simplicity at the watershed scale: is there a connection? *Hydrological Processes* **17**(5): 1037–1041. DOI:10.1002/hyp.5109.
Sivapalan M, Beven K, Wood WF. 1987. On hydrologic similarity: a scaled model of storm runoff production. *Water Resources Research* **23**(12): 2266–2278. DOI:10.1029/WR023i012p02266.
Swedish Hydrological Modeling Institute. 2005. HBV-IHMS software manual version 5·1.
Sorooshian S, Hsu KL, Coppola E, Tomassetti B, Verdecchia M, Visconti G (eds). 2008. *Hydrological modeling and the water cycle: coupling the atmospheric and hydrological models*, Vol. **63**. Springer Heidelberg Berlin: California, USA; 1–25.
Steenhuis TS, Collick AS, Easton ZM, Leggesse ES, Bayabil HK, White ED, Awulachew SB, Adgo E, Ahmed AA. 2009. Predicting discharge and sediment for the Abay (Blue Nile) with a simple model. *Hydrological Processes* **23**(26): 3728–3737. DOI:10.1002/hyp.7513.
Steenhuis TS, van der Molen WH. 1986. Thornthwaite–Mather procedure as a simple engineering method to predict recharge. *Journal of Hydrology* **84**: 221–229. DOI:10.1016/0022-1694(86)90124-1.
Taddese G. 2001. Land degradation: a challenge to Ethiopia. *Environmental Management* **27**(6): 815–824. DOI:10.1007/s002670010190.
Tebebu TY, Steenhuis TS, Dagnew DC, Guzman CD, Bayabil HK, Zegeye AD, Collick AS, Langan S, McAllister C, Langendoen EJ, Yitaferu B, Tilahun SA. 2015. Improving efficacy of landscape interventions in the (sub) humid Ethiopian Highlands by improved understanding of runoff processes. *Frontiers in Earth Science* **3**: 49. DOI:10.3389/feart.2015.00049.
Tesemma ZK, Mohamed YA, Steenhuis TS. 2010. Trends in rainfall and runoff in the Blue Nile basin: 1964–2003. *Hydrological Processes* **24**: 3747–3758. DOI:10.1002/hyp.7893.
Tilahun SA, Ayana EK, Guzman CD, Dagnew DC, Zegeye AD, Tebebu TY, Yitaferu B, Steenhuis TS. 2016. Revisiting storm runoff processes in the Upper Blue Nile basin: the Debre Mawi watershed. *CATENA* **143**: 47–56.
Tilahun SA, Guzman CD, Zegeye AD, Dagnew DC, Collick AS, Yitaferu B, Steenhuis TS. 2015. Distributed discharge and sediment concentration predictions in the sub-humid Ethiopian Highlands: the Debre Mawi watershed. *Hydrological Processes* **29**(7): 1817–1828. DOI:10.1002/hyp.10298.
Tilahun SA, Guzman CD, Zegeye AD, Ayana EK, Collick AS, Yitaferu B, Steenhuis TS. 2014. Spatial and temporal patterns of soil erosion in the semi-humid Ethiopian Highlands: a case study of Debre Mawi watershed. In *Nile River Basin: Ecohydrological Challenges, Climate Change and Hydropolitics*, Assefa M, Abtew W, Setegn SG (eds). Springer: Cham Heidelberg, New York, Dortrecht, London; 149–164. DOI: 10.1002/hyp.7457.
Tilahun S, Guzman C, Zegeye A, Engda T, Collick A, Rimmer A, Steenhuis T. 2013a. An efficient semi-distributed hill slope erosion model for the sub-humid Ethiopian Highlands. *Hydrology and Earth System Sciences* **17**(3): 1051–1063. DOI:10.5194/hess-17-1051-2013.
Tilahun SA, Mukundan R, Demisse BA, Engda TA, Guzman CD, Tarakegn BC, Easton ZM, Collick AS, Zegeye AD, Schneiderman EM, Parlange JY, Steenhuis TS. 2013b. A saturation excess erosion model. *ASABE* **56**: 681–695. DOI:10.13031/2013.42675.
Tilahun SA, Guzman CD, Zegeye AD, Engda TA, Collick AS, Rimmer A, Steenhuis TS. 2012. An efficient semi-distributed hillslope erosion model for the sub humid Ethiopian Highlands. *Hydrology and Earth System Sciences Discussions* **9**(2): 2121–2155. DOI:10.5194/hessd-9-2121-2012.
Todini E. 1996. The ARNO rainfall–runoff model. *Journal of Hydrology* **175**(1-4): 339–382. DOI:10.1016/S0022-1694(96)80016-3.
VanShaar JR, Haddeland I, Lettenmaier DP. 2002. Effects of land-cover changes on the hydrological response of interior Columbia River basin forested catchments. *Hydrological Processes* **16**(13): 2499–2520. DOI:10.1002/hyp.1017.
Van GA, Meixner T, Bishop T, Diluzio A, Srinivasesn R. 2006. A global sensitivity analysis tool for parameters of multi-variable catchment models. *Journal of Hydrology* **324**(1-4): 10–23. DOI:10.1016/j.jhydrol.2005.09.008.
Wale A, Rientjes THM, Gieske ASM, Getachew HA. 2009. Ungauged catchment contributions to Lake Tana water balance. *Hydrological Processes* **23**(26): 3682–3693. DOI:10.1002/hyp.7284.
Wang Y, Fan J, Cao L, Liang Y. 2015. Infiltration and runoff generation under various cropping patterns in the red soil region of China. *Land Degradation and Development* **27**(1): 83–91. DOI:10.1002/ldr.2460.
Wessels KJ, Prince SD, Frost PE, Van ZD. 2004. Assessing the effects of human-induced land degradation in the former homelands of northern South Africa with a 1 km AVHRR NDVI time-series. *Remote Sensing of Environment* **91**(1): 47–67. DOI:10.1016/j.rse.2004.02.005.
Wheater HS, Bishop KH, Beck MB. 1986. The identification of conceptual hydrological models for surface water acidification. *Hydrological Processes* **1**: 89–109. DOI:10.1002/hyp.3360010109.
Young WJ, Marston FM, Davis RJ. 1996. Nutrient exports and land use in Australian catchments. *Journal of Environmental Management* **47**(2): 165–183. DOI:10.1006/jema.1996.0043.
Zeleke G, Hurni H. 2001. Implications of land use and land cover dynamics for mountain resource degradation in the Northwestern Ethiopian highlands. *Mountain Research and Development* **21**(2): 184–191.

SUPPORTING INFORMATION

Additional supporting information may be found in the online version of this article at the publisher's web site:

Figure S1. Stage discharge relationship at the outlet of Awramba watershed.
Table S1. Input data used by each of watershed model for Awramba watershed.
Table S2. Sub-basins based on HBV-IHMS model for the Awramba watershed.
Table S3. HRUs based on SWAT model for the Awramba watershed.
Table S4. SWAT parameters used for calibration with the fitted values and sensitivity ranks.